Quantitative Measurement of 3D Tumor Spheroid Invasion Using Live Cell Time-Lapse Imaging

Grace Yang, Tian Wang, Peifang Ye, Xiaoyu Zhang

Agilent Technologies, Inc.

SITC2025 #147

Agilent Trusted Answers

Introduction

Ninety percent of the deaths of cancer individuals are related to cancer metastasis.[1] The invasion and migration of cancer cells into surrounding tissues and chambers is the first step of **metastasis.**[2]

To have a better and more in-depth understanding of the pathophysiological activities involved in metastatic cancer, accurate and reliable methods for evaluating cell invasion are urgently needed.

Compared to the 2D cell model, the 3D system mimics the natural physiological properties and conditions, such as structure, physiology, biological signals of living tissues, and cell-matrix interactions.[3]

Combining the **3D tumor spheroid invasion** model with the **Agilent xCELLigence RTCA eSight** capability of **live-cell imaging and automatic quantification of the area of invasive protrusion** can facilitate and enhance the development of new treatments at the preclinical stage in the future.

Experimental Design

Brief workflow of 3D spheroid invasion assay using xCELLigence RTCA eSight system.

Day 0 - 3	Day 3	Day 3 -10
1. Seed target cells (150 µL/well) into 96-well round bottom ultra-low attachment microplates (Corning, p/n 7007). Centrifuge. 2. Place the plate inside the xCELLigence RTCA eSight and scan every four hours for 3 days to monitor the formation of spheroids.	1. Gently remove 120 µL media and add 50 µL Matrigel (5 mg/mL, with 1x compound) subsequently. 2. Polymerize at 37°C for 30 min. 3. Add 100 µL compound-containing medium on top of Matrigel.	1. Place the plate back in the Agilent xCELLigence RTCA eSight system. 2. Monitor spheroid invasion every four hours for up to 10 days.

Key parameters used for 3D spheroid invasion assay

The reliability of the 3D in vitro tumor spheroid invasion model for assessing the inhibitory effect of metastasis depends on its ability to identify the spheroid invasion area.

1. **Invading cell area** is defined by the total area of the spheroid at time t (following treatment) subtracting the total area of the spheroid at time t0 (initial area, the area right after the addition of Matrigel and compound).[4]

$$Invading\ cell\ area = Area_t - Area_{t0}$$

2. **Invading ratio** is defined as the ratio of the invasion area to the initial area of the spheroid.

$$Invading\ ratio = \frac{Area_t - Area_{t0}}{Area_{t0}}$$

Results and Discussion

Different cell lines exhibit various levels of invasion capability.

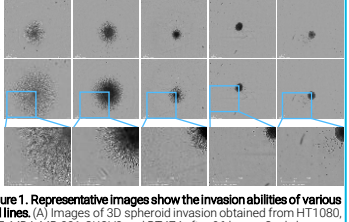

Figure 1. Representative images show the invasion abilities of various cell lines. (A) Images of 3D spheroid invasion obtained from HT1080, U87, MDA-MB-231, SKOV3 and BT474 after 96 hours. Scale bar, 300 µm. (B) Close-up Images from each cell type.

Cytochalasin D dose-dependently inhibits HT-1080 spheroid invasion through brightfield recognition.

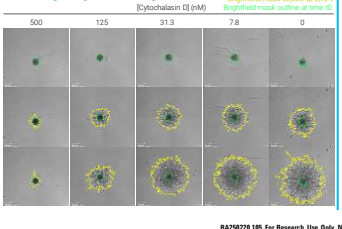

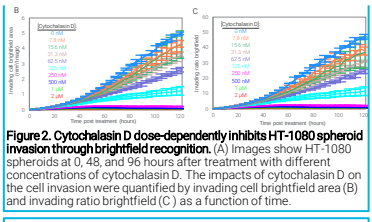

Figure 2. Cytochalasin D dose-dependently inhibits HT-1080 spheroid invasion through brightfield recognition. (A) Images show HT-1080 spheroids at 0, 48, and 96 hours after treatment with different concentrations of cytochalasin D. The impacts of cytochalasin D on the cell invasion were quantified by invading cell brightfield area (B) and invading ratio brightfield (C) as a function of time.

Cytochalasin D dose-dependently inhibits HT-1080 spheroid invasion through fluorescence recognition.

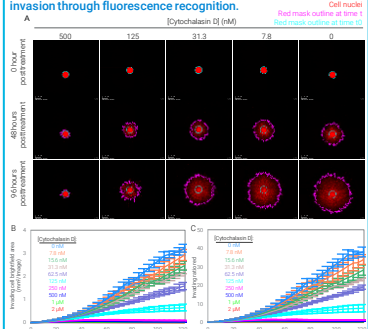

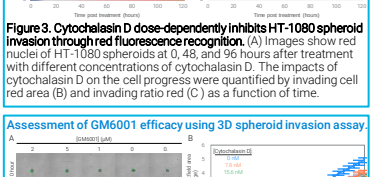

Figure 3. Cytochalasin D dose-dependently inhibits HT-1080 spheroid invasion through red fluorescence recognition. (A) Images show red nuclei of HT-1080 spheroids at 0, 48, and 96 hours after treatment with different concentrations of cytochalasin D. The impacts of cytochalasin D on the cell progress were quantified by invading cell red area (B) and invading ratio red (C) as a function of time.

Assessment of GM6001 efficacy using 3D spheroid invasion assay.

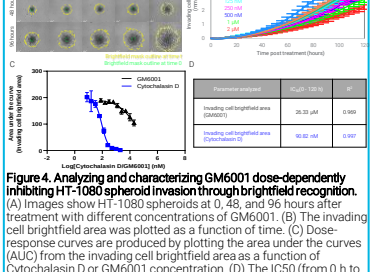

Parameter analyzed	IC_{50} (0 - 120 h)	R^2
Invading cell brightfield area (GM6001)	26.33 µM	0.969
Invading cell brightfield area (Cytochalasin D)	90.82 nM	0.997

Figure 4. Analyzing and characterizing GM6001 dose-dependently inhibiting HT-1080 spheroid invasion through brightfield recognition. (A) Images show HT-1080 spheroids at 0, 48, and 96 hours after treatment with different concentrations of GM6001. (B) The invading cell brightfield area was plotted as a function of time. (C) Dose-response curves are produced by plotting the area under the curves (AUC) from the invading cell brightfield area as a function of Cytochalasin D or GM6001 concentration. (D) The IC50 (from 0 h to 120 h posttreatment) values of cytochalasin D or GM6001 were derived from dose-response curves in (C).

Conclusions

Different types of cancer cells had different metastatic potentials demonstrated by the level of invadopodium extending into the Matrigel at desired time points;

The invasion of 3D HT1080 spheroid was inhibited by cytochalasin D, an inhibitor of actin polymerization, and GM6001, a potent broad-spectrum inhibitor of matrix metalloproteinases (MMP), in a dose-dependent manner;

Cytochalasin D exhibited higher efficacy in inhibiting tumor invasion than GM6001.

Combining the 3D tumor spheroid invasion model with the Agilent xCELLigence RTCA eSight capability of live-cell imaging and automatic quantification of the area of invasive protrusion can facilitate and enhance the development of new treatments at the preclinical stage in the future.

References

1. Steeg, P. S. Tumor metastasis: mechanistic insights and clinical challenges. *Nat. Med.* **2006**, *12*(8), 895-904. DOI: 10.1038/nm1469

2. Modi, U.; Makwana, P.; Vasita, R. Molecular insights of metastasis and cancer progression derived using 3D cancer spheroid co-culture in vitro platform. *Cnt Rev. Oncol. Hematol.* **2021** 168, 103511. DOI: 10.1016/j.critrevonc.2021.103511

3. Costa, E.C.; Moreira, A.F.; de Melo-Diogo, D.; Gaspar, V.M.; Carvalho, M.P.; Correia, I.J. 3D tumor spheroids: an overview on the tools and techniques used for their analysis. *Biotechnol. Adv.* **2016**, 34(8), 1427-1441. DOI: 10.1016/j.biotechadv.2016.11.002.

4. Vinci, M.; Box, C.; Eccles, S.A. Three-dimensional (3D) tumor spheroid invasion assay. *J Vis Exp.* **2015**, 99 e52686. DOI: 10.3791/52686.